Distortion of terahertz signals due to imperfect synchronization with chirped probe pulses

Xiao-Yu Peng,[1,*] Zheng-Ming Sheng,[2] Xin-Hai Zhang,[1] Jing-Hua Teng,[1] Hong-Cheng Guo,[1] Yong-Lim Foo,[1] and Jie Zhang[2]

[1]Institute of Materials Research and Engineering (IMRE), Agency for Science, Technology and Research (A*STAR), 3 Research Link, 117602 Singapore, Singapore
[2]Key Laboratory for Laser Plasmas (Ministry of Education) and Physics Department, Shanghai Jiaotong University, Shanghai 200240, China
*Corresponding author: pengxy@imre.a-star.edu.sg

Received June 28, 2011; revised August 11, 2011; accepted August 12, 2011; posted August 24, 2011 (Doc. ID 149701); published September 12, 2011

Terahertz (THz) signals measured by means of the spectral-encoding technique with different temporal discrepancies between probe pulses and THz signals are investigated. It is found that imperfect synchronization between the chirped probe and THz pulses induce a distortion and this distortion affects significantly the retrieved THz spectrum if the temporal discrepancy is large. The distortion becomes more prominent if the probe pulse length is less than the optimal chirped probe pulse duration. A simple approach is proposed to realize the synchronization and minimize the distortion. THz signals from a high-voltage-biased air plasma filament are measured with this approach and distortion similar to the simulation results is observed.

OCIS codes: 300.6495, 320.7100, 350.5400, 350.5610.

1. INTRODUCTION

Terahertz (THz) detection techniques have been developed rapidly in the past two decades due to the requirements of numerous applications of THz science and technology. The conventional detection technique for THz pulses or T-rays, called electro-optic sampling (EOS) [1], is a scanning technique. Through EOS, the electric field profile including the phase and amplitude of a THz pulse can be measured. This is a mature technique suitable for THz sources with high repetition rates, generally not less than 1 kHz. However, EOS is not suitable to be applied in some cases, such as T-rays with low repetition rates or with strong shot-to-shot fluctuations. Consequently, single-shot detection techniques or methods have been proposed in recent years, and they include the spectral-encoding technique [2], using an optical streak camera instead of the spectrometer [3], the interferometric retrieval algorithm [4,5], the spatial encoding technique [6], the cross-correlation technique [7], two-dimensional EO imaging with dual echelons [8], using pulse-front tilting by a direct vision dispersion prism [9], and utilizing a stretched supercontinuum optical pulse as the probe pulse [10]. Among these single-shot techniques, the spectral-encoding technique is one of the most convenient and most sensitive ones due to its simple optical arrangement, easy retrieving process, requirement of only small laser energy ($\sim 1\,\mu$J or less) for the probe pulse, and operation in real time.

Just like other single-shot techniques, the spectral-encoding technique has its own intrinsic disadvantages. The main disadvantage of this technique is that distortions will be induced if some conditions are not satisfied. In previous work [11,12], the main distortion of this technique was attributed to the low temporal resolution of the detection system, namely, $T_{\min} \approx (T_0 T_c)^{1/2}$, where T_0 is the original probe pulse length and T_c is the chirped probe pulse length. Afterward, a rigorous relationship [13] between the probe pulse length and the bipolar THz pulse length was found. It indicates that there is an optimal chirped probe pulse length T_{co} (or an optimal chirp rate) that matches the input THz pulse length T and only under this restricted condition can the THz signal be properly retrieved. Besides this main distortion due to $T_c \neq T_{\mathrm{co}}$, two other kinds of distortion, namely, the distortion from the strong THz signal when the modulation depth $k \ll 1$ is not satisfied [14,15] and the distortion relevant to the spectral bandwidth of the probe pulse [15], not only for single-cycle THz waveforms but also for multicycle THz waveforms, were recently analyzed in detail. However, all analyses and discussions were based on an assumption that the probe pulse was perfectly synchronized with the THz pulse. In practice, it is difficult to judge two pulses to be exactly synchronized if evaluated only according to the modulated probe spectrum. A possible popular incorrect impression is that the detected strongest signal corresponds to perfect synchronization. However, our investigation proves that it is not true. If the probe pulse is not synchronized perfectly with the THz pulse, a new distortion is introduced. So far, we have found no publications that discuss how the imperfect synchronization affects the retrieved THz signal. In this article, we demonstrate the distortion of detected THz signals with the spectral-encoding technique due to imperfect synchronization between the chirped probe pulse and the THz pulse numerically and experimentally. Also, a simple approach is proposed to minimize the distortion.

2. NUMERICAL SIMULATION

For the sake of simplicity, the THz signal retrieving process was simulated numerically by assuming the input THz signal as a simple bipolar THz waveform $E_{\mathrm{THz}}(t) = tT^{-1}\exp(-t^2T^2)$; here we define a characteristic time $2^{1/2}T$ that is the interval between the maximum and the minimum. The electric field component of the original probe pulse with a central frequency ω_0 and a Gaussian envelope can be written as $E_0(t) = \exp(-t^2T_0^{-2} - i\omega_0 t)$. Here T_0 is the pulse length, which is related to the laser spectral bandwidth $\Delta\omega_0$ through $T_0 = 2/\Delta\omega_0$. After stretching by a grating pair or a dispersive glass, the electric field component of the probe pulse can be written as $E_c(t) = \exp(-t^2T_c^{-2} - i\alpha t^2 - i\omega_0 t)$, where T_c is the pulse length after chirping, and 2α is the chirp rate, which is approximated as the laser bandwidth divided by the chirped laser pulse length, i.e., $2\alpha \approx \Delta\omega_0/T_c$. Considering that the polarizer and the analyzer are crossed exactly to each other and without wave plate or analyzer detuning, the electric field of the chirped probe pulse modulated by the THz field can be expressed as

$$E_m(t) = E_c(t)[1 + kE_{\mathrm{THz}}(t - \Delta t)]. \tag{1}$$

Here, k is the modulation depth or modulation constant, which reflects the strength of the THz field, and Δt is the relative time delay or temporal discrepancy between the probe pulse and the THz pulse. When $\Delta t > 0$, the probe pulse lags behind the THz pulse, whereas the probe pulse leads the THz pulse when $\Delta t < 0$. One may obtain the background probe spectrum I_b and the modulated probe spectrum I_m by calculating the square of the Fourier transform of $E_c(t)$ and $E_m(t)$. The THz waveform can be retrieved from the spectrum difference $\Delta I = I_m - I_b$ with a simple coordinate transformation $\omega_1 - \omega_0 = 2\alpha t$, where ω_1 corresponds to the frequency of the chirped probe spectrum. A more detailed theory for the THz retrieving process can be found in [13,15]. Given an input THz signal with a characteristic time $2^{1/2}T$ (or dimensionless pulse length $m = T/T_0$), the corresponding optimal chirped pulse length T_{co} can be calculated with the following equation [13]:

$$T_{\mathrm{co}} = \left\{\frac{1}{3}\left[2(6m^6 + 4m^4 - 8m^2 + 1)^{1/2}\cos\left(\frac{\beta}{3}\right) - (m^2 - 1)\right]\right\}^{1/2} T_0, \tag{2}$$

where

$$\beta = \arccos\left[-\frac{3}{54}\frac{18m^8 + 61m^6 + 6m^4 + 24m^2 - 2}{(6m^6 + 4m^4 - 8m^2 + 1)^{3/2}}\right].$$

Assuming $T_0 = 36\,\mathrm{fs}$ and $T = 0.5\,\mathrm{ps}$, the corresponding optimal chirped probe pulse duration T_{co} is 2.198 ps, which is calculated according to Eq. (2). First, we consider only the case where the probe pulse length equals exactly the optimal probe pulse duration, i.e., $T_c = T_{\mathrm{co}}$. The simulation results with parameters $\alpha > 0$ and $k = 0.05$ are shown in Fig. 1. The modulated spectra I_m under the conditions of different temporal discrepancy Δt versus the background probe spectrum I_b are shown in Fig. 1(a). The vertical dashed lines indicate the central wavelength λ_c ($= 800\,\mathrm{nm}$) of the background I_b. One may observe that the peak of I_m, namely, $\max(I_m)$, tends to the maximum when $\Delta t = -T$ and to the minimum when $\Delta t = T$, respectively. However, it is difficult to distinguish the modulated spectrum when $\Delta t = 0$ from others. In other words, it is hard to judge if the probe pulse is synchronized perfectly with the THz pulse directly from the modulated probe spectrum. If we calculate the spectrum difference $\Delta I = I_m - I_b$ as shown in Fig. 1(b), the situation becomes more clear. One can observe that the positive pole and the negative pole of the curve ΔI distribute symmetrically with respect to the grid origin of central wavelength $(800\,\mathrm{nm}, 0)$ when $\Delta t = 0$, as shown by the dashed curve in Fig. 1(b). The strongest positive peak or the negative peak of ΔI does not correspond to the perfect synchronization $\Delta t = 0$, but corresponds to $\Delta t = -T$ or T. This result can be observed more conveniently in Fig. 1(c), which shows the positive and negative peaks of the spectrum difference ΔI shown in Fig. 1(b). Furthermore, one can find that the larger the temporal discrepancy $|\Delta t|$, the smaller the ΔI will be, or the smaller part of the spectrum is modulated by the THz signal. The temporal THz signals at different temporal discrepancy Δt are retrieved from the spectrum difference normalized to the peak value of background, i.e., $\Delta I/\max(I_b)$, and are shown in Fig. 1(d). The positive and negative peaks of the retrieved temporal THz signals are shown in Fig. 1(e). One may find that the strongest strength of THz signal does not correspond to the perfect synchronization between the probe and the THz pulses from Figs. 1(d) and 1(e). The corresponding spectra of retrieved temporal THz signals are shown in Fig. 1(f). From Figs. 1(d) and 1(f), it is clear that the retrieved THz waveform matches the original input signal very well only when the probe is synchronized perfectly with the THz pulse ($\Delta t = 0$). The larger the discrepancy Δt, the more severe the distortion of the THz waveform and its spectrum will be. In the cases of $\Delta t = \pm 4T$, nearly only one pole of the THz waveform is recorded by the spectrometer. From Fig. 1(f), one can observe that the THz spectrum is redshifted with the increase of $|\Delta t|$: the larger the $|\Delta t|$, the more the spectral intensity increases at low frequencies and decreases at high frequencies.

For the symmetric bipolar THz signal, fortunately, the distortion is small if the time discrepancy $|\Delta t| \le T$ ($T = 0.5\,\mathrm{ps}$), as shown in Fig. 1(f). In practice, because most THz signals have an arbitrary shape, like a multicycle or asymmetric bipolar THz waveform, it would be more difficult to judge if two pulses are synchronized perfectly. Figure 2 shows an example of arbitrary THz waveform similar to an asymmetric bipolar THz signal, with its pulse length close to that of the bipolar THz signal length shown in Fig. 1. The original THz signal is mimicked with following model:

$$E_{\mathrm{thz}}(t) = \frac{t - T/x - T}{T}\exp\left[-\frac{2(t - T/x - T)^2}{T^2}\right] \times \exp\left[-\frac{8(t - T/x - T)}{xT}\right]\cos\left[2\pi\left(\frac{t - T/x - T}{xT}\right)\right].$$

Here $x = 2$, $T = 1.3\,\mathrm{ps}$, and $T_{\mathrm{co}} \sim 2.7\,\mathrm{ps}$. Parameters of the probe pulse are the same as in Fig. 1. The modulated probe spectra and the spectrum difference ΔI between the modulated probe spectra and the background are shown in Figs. 2(a) and 2(b), respectively. Comparing with the case of a symmetric bipolar THz signal, one finds that it is more difficult to judge when two pulses are synchronized to each other exactly, as shown in Figs. 2(a) and 2(b). To see clearly the dependence of ΔI on the time discrepancy Δt, the positive and negative peaks of ΔI are shown in Fig. 2(c). One finds that, just like the case of a bipolar THz waveform, the

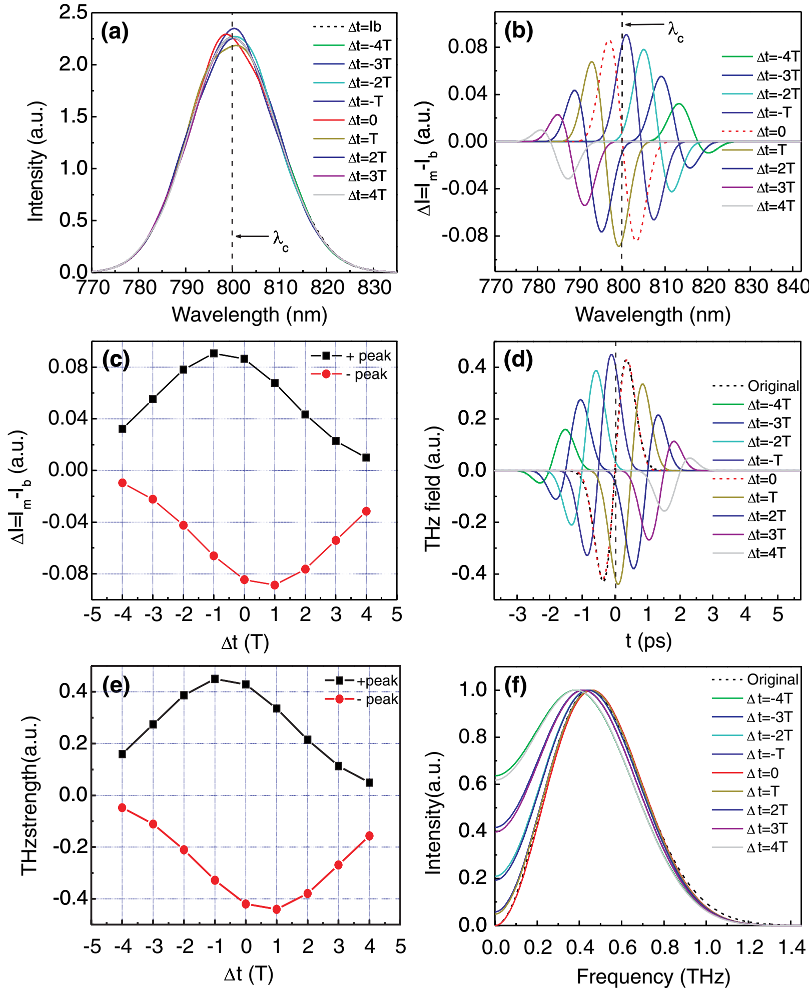

Fig. 1. (Color online) Simulation results of the THz signals measured with optimal chirped probe pulse length ($T_c = T_{co}$) at different temporal discrepancy Δt. (a) Modulated spectra I_m versus background I_b at different Δt; (b) spectrum difference $\Delta I = I_m - I_b$ at different Δt; (c) the positive and negative peaks of spectrum difference ΔI at different Δt; (d) retrieved THz waveforms at different Δt; (e) the positive and negative peaks of retrieved THz waveforms at different Δt; (f) retrieved THz spectra at different Δt. In the simulation, $T_0 = 0.36\,\text{ps}$, $T = 0.5\,\text{ps}$, and $T_{co} = 2.198\,\text{ps}$. The vertical dashed lines in (a) and (b) indicate the central wavelength λ_c of the background probe spectrum I_b.

strongest signal does not correspond to the perfect synchronization ($\Delta t = 0$). This conclusion can be further proved by the retrieved THz temporal waveforms and their positive and negative peaks at different Δt, as shown in Figs. 2(d) and 2(e), respectively. The above simulation results indicate that the strongest signal is not a good criterion for judging if the probe pulse is synchronized perfectly with the THz pulse. The spectra of THz signals are shown in Fig. 2(f). One observes that even a small time discrepancy, for example, $\Delta t = \pm 0.3T = \pm 0.39\,\text{ps}$, could possibly induce significant distortion as, shown in Figs. 2(d) and 2(f). The behavior of the THz spectrum becomes more complicated than that in the case of symmetric bipolar THz signals: the THz spectrum is redshifted when $\Delta t < 0$, but is blueshifted when $\Delta t > 0$.

The above simulation is based on the assumption that the optimal chirped probe pulse length is applied, i.e., $T_c = T_{co}$. However, generally, the probe pulse length is not exactly equal to T_{co} in practice. To see that the behavior of the distortion originates from imperfect synchronization in the case that the optimal chirped probe pulse length is not used, we simulated the bipolar THz signal retrieving processes in the cases of $T_c = 0.7T_{co}$ and $T_c = 1.4T_{co}$ at different temporal discrepancy Δt. The simulation results are shown in Fig. 3. One may find that the retrieved THz signals do not match the original ones very well, even in cases of perfect synchronization ($\Delta t = 0$). This distortion comes from the mismatch $T_c \neq T_{co}$, which has been discussed in detail in previous work [13,15]. In other cases ($\Delta t \neq 0$), one may observe that, with the same discrepancy Δt, compared with the case of $T_c = T_{co}$ as shown in Fig. 1(c), the curve of ΔI moves more in the case of $T_c = 0.7T_{co}$, as shown in Fig. 3(a), and moves less in the case of $T_c = 1.4T_{co}$, as shown in Fig. 3(d). With the same temporal discrepancy $\Delta t = \pm 4T$, only a small part of the THz signal is detected by the spectrometer in the case of $T_c = 0.7T_{co}$, while most of the THz signal is still detected by the spectrometer in the case of $T_c = 1.4T_{co}$. These phenomena are also reflected from the retrieved temporal THz signals, as shown in Figs. 3(b) and 3(e). Furthermore, comparing Figs. 3(c) and 3(f) with Fig. 1(f), with the same temporal discrepancy Δt, one finds that the lower frequency part is increased more and the higher frequency part is suppressed more in the case of $T_c = 0.7T_{co}$, while the lower frequency part is increased less and the higher frequency part is suppressed less in the case of $T_c = 1.4T_{co}$. More simulation for arbitrary THz

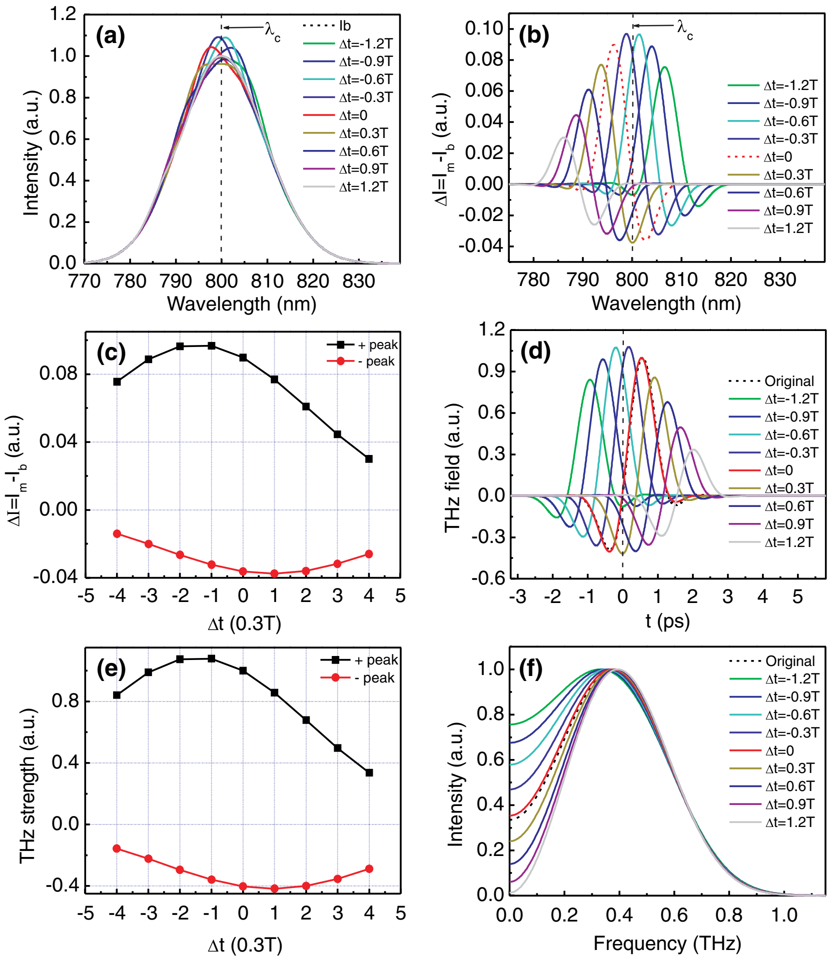

Fig. 2. (Color online) Simulation results of the arbitrary THz signals measured with optimal chirped probe pulse lengths ($T_c = T_{co}$) at different temporal discrepancy Δt. (a) Modulated spectra I_m versus background I_b at different Δt; (b) spectrum difference $\Delta I = I_m - I_b$ at different Δt; (c) the positive and negative peaks of spectrum difference ΔI at different Δt; (d) retrieved THz waveforms at different Δt; (e) the positive and negative peaks of retrieved THz waveforms at different Δt; (f) retrieved THz spectra at different Δt. In the simulation, $T_0 = 0.36$ ps, $T = 0.7$ ps, and $T_{co} \sim 2.7$ ps. The vertical dashed lines in (a) and (b) indicate the central wavelength λ_c of the background probe spectrum I_b.

waveforms was performed and similar phenomena were observed. In short, from Fig. 3, one may conclude that the distortion due to imperfect synchronization between the probe and THz pulses becomes more severe if the probe pulse length T_c is less than the optimal probe pulse length T_{co}, while it is less severe if the probe pulse length T_c is longer than the optimal probe pulse length T_{co}.

3. EXPERIMENTAL RESULTS

To further understand the behavior of the distortion due to imperfect synchronization, we performed an experiment to measure the THz signals with the spectral-encoding technique under the condition of different delays. For the sake of convenient contrast with the simulation results illustrated in Section 2, the THz source was generated from a high-voltage dc-biased air plasma filament. This radiation has a quasi-bipolar waveform [16,17], similar to the shape shown in Fig. 2, with different amplitudes of the negative and the positive polars.

The schematic of our experimental setup is shown in Fig. 4. A commercial Ti:sapphire amplified laser system delivered 36 fs duration pulses with a center wavelength of 800 nm, operating at a repetition rate of 1 kHz. The laser beam was separated into two beams by a beam splitter: one beam with most of the pulse energy was used as the pump and the other one with a small amount of the pulse energy was used as the probe. The pump pulses with typical energy 2.9 mJ per pulse were focused in air by a converging lens ($f/20$) to form a plasma filament. A static electric field with high voltage of −18 kV was applied to the ionized region by two copper plane electrodes with 1 cm distance across the filament. THz radiation from the filament was collimated and focused by a couple of OAP mirrors to the surface of an electro-optical crystal (ZnTe with thickness of 1 mm). A silicon wafer was inserted between two OAP mirrors to filter the residual laser light and the visible light from the plasma emission. The THz detection system consisted of dispersive glasses, a couple of crossed polarizers, and a fiber spectrometer (Avaspec 2048). The dispersive glasses included two parts: an SF66 glass brick with fixed length of 5 cm and a pair of triangular SF57 prisms with adjustable lengths from ~5 to ~11 cm, which was dependent on the sizes of both prisms and the range of the stage for supporting the pair prism. This group of dispersive glasses could stretch the original probe pulse ($T_0 = 36$ fs) and provided a chirped probe pulse length ranging from ~2 to ~3 ps. The combined glasses have more advantages over a pair of gratings because they are able to adjust continuously the chirp rate of the probe pulse by moving one of the SF57 pair

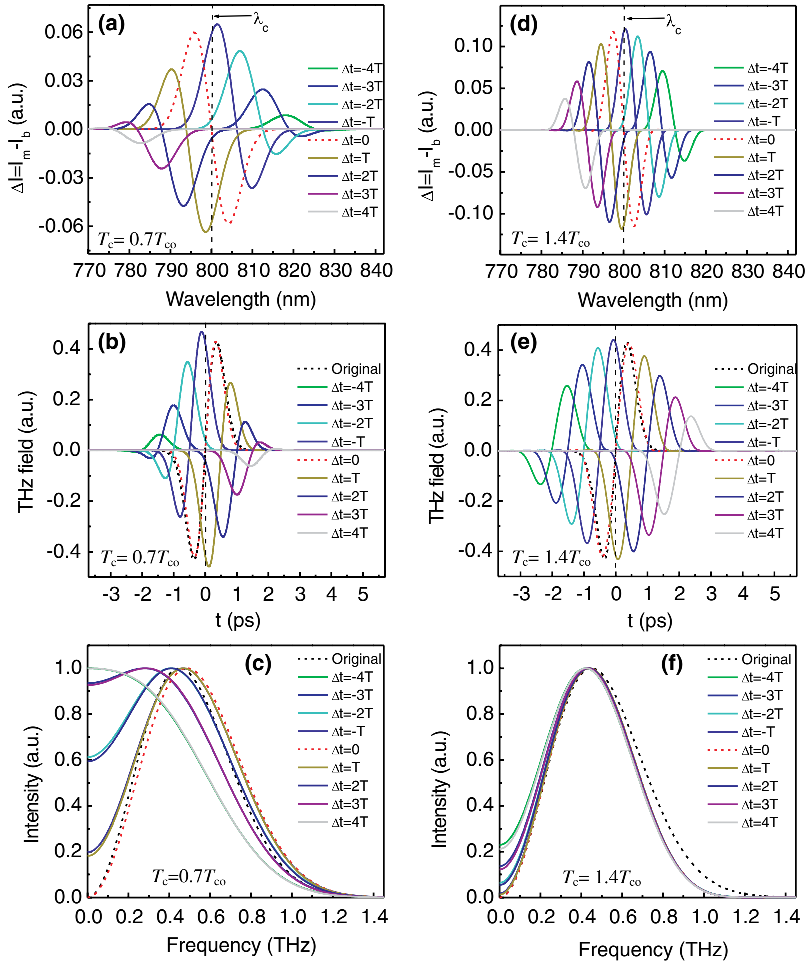

Fig. 3. (Color online) Simulation results of the THz signals measured with nonoptimal chirped probe pulse lengths $T_c = 0.7T_{co}$ and $T_c = 1.4T_{co}$ at different temporal discrepancy Δt. (a) and (d) Spectrum difference $\Delta I = I_m - I_b$ at different Δt; (b) and (e) retrieved THz waveforms at different Δt; (c) and (f) retrieved THz spectra at different Δt. In the simulation, $T_0 = 0.36$ ps, $T = 0.5$ ps, and $T_{co} = 2.198$ ps. The vertical dashed lines in (a) and (d) indicate the central wavelength λ_c of the background probe spectrum I_b.

prisms without the shift of the probe beam, while moving one of a pair gratings would shift the probe beam. Also, it is easy to calculate the chirp rate according to the glass parameters and the length. Considering the fluctuation of the laser pulses, the integration time, the number of averages, and the spectrum smooth factor of the fiber spectrometer were set to 20 ms, 20 times and 10, respectively. The temporal discrepancy Δt between the probe pulse and the THz pulse was adjusted with the same increment of t_0 step by step by moving a probe beam delay stage, as shown in Fig. 4. The length of the SF57 pair prism was adjusted to 8 cm. The total chirp rate of the probe pulse was $3.144 \times 10^{25}\ \mathrm{s}^{-2}$, which was calculated according to the parameters of the SF66 and SF57 glasses. Hence, the duration of the chirped probe pulse was ~2.5 ps. Considering that the THz signal has an asymmetric bipolar waveform, it would change more sensitively under the same temporal discrepancy Δt compared with the symmetric bipolar THz waveform discussed in the above simulations. Therefore, the delay increment $t_0 = 0.1334$ ps was set to be smaller than that in the

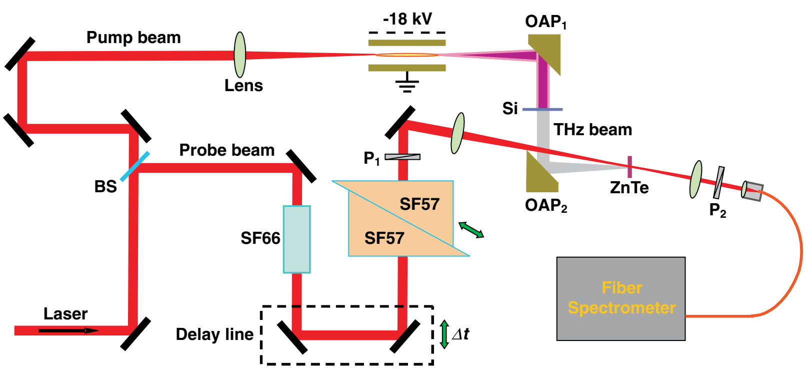

Fig. 4. (Color online) Schematic of experimental setup with the detection system of the spectral-encoding technique.

simulations in order to see clearly the distortion behavior of the THz signals.

The experimental results are shown in Fig. 5. The results show similar behavior as that of the simulation results shown in Fig. 2. The modulated probe spectra versus background probe spectrum I_b at different temporal discrepancy Δt are shown in Fig. 5(a). Just like in the cases shown in Figs. 1(a) and 2(a) of the simulation results, it is difficult to distinguish the modulated probe spectrum at perfect synchronization ($\Delta t = 0$) between the probe pulse and the THz pulse directly from other spectra with temporal discrepancy ($\Delta t \neq 0$). The peak of the modulated spectrum I_m tends to the minimum at $\Delta t = -2t_0$ and to the maximum at $\Delta t = 3t_0$. But the increment of I_m at $\Delta t = 3t_0$ is nearly twice larger than the decrease of I_m at $\Delta t = -2t_0$. This is attributed to the positive polar of the THz signal, which is ~2 times stronger than its negative polar. After saving a background spectrum I_b and setting "Subtract saved dark" in the software of the fiber spectrometer, we easily obtained the spectrum difference ΔI at different temporal discrepancy in real time, as shown in Fig. 5(b), and the positive and the negative peaks of ΔI shown in Fig. 5(c). The dashed red curve of ΔI corresponds to the case of perfect synchronization ($\Delta t = 0$). One observes that the curve of ΔI moves more when $\Delta t > 0$ than that when $\Delta t < 0$ with the same Δt, which is due to the same reason that the amplitude of the positive polar of the THz signal is larger than its negative polar. The THz waveforms and their frequency spectra are shown in Figs. 5(d) and 5(f), retrieved from the normalized spectrum difference $\Delta I/\max(I_b)$. Also, the positive and negative peaks of the temporal THz signals are shown in Fig. 5(e). One can see clearly that the positive peak of the THz signal is ~2 times stronger than its negative peak for perfect synchronization ($\Delta t = 0$). The larger the temporal discrepancy Δt, the more distorted the THz waveform and its spectrum will be. Especially in the cases of $\Delta t > t_0$, the retrieved THz field becomes stronger and stronger; however, in practice, nearly only the positive polar of the THz waveform was recorded by the spectrometer. As a result, the corresponding spectra have a very severe distortion, as shown in Fig. 5(f). The larger the temporal discrepancy when $\Delta t > 0$, the more severe the distortion will be. From Fig. 5(f), one may clearly observe that the retrieved THz spectrum is redshifted when $\Delta t < 0$, while it is blueshifted when $\Delta t > 0$, similar to the simulation results shown in Fig. 2(f).

It should be noted that the THz spectrum curves appear not smooth in Fig. 5(f). This is mainly due to the low temporal resolution of the retrieved THz pulse shown in Fig. 5(d),

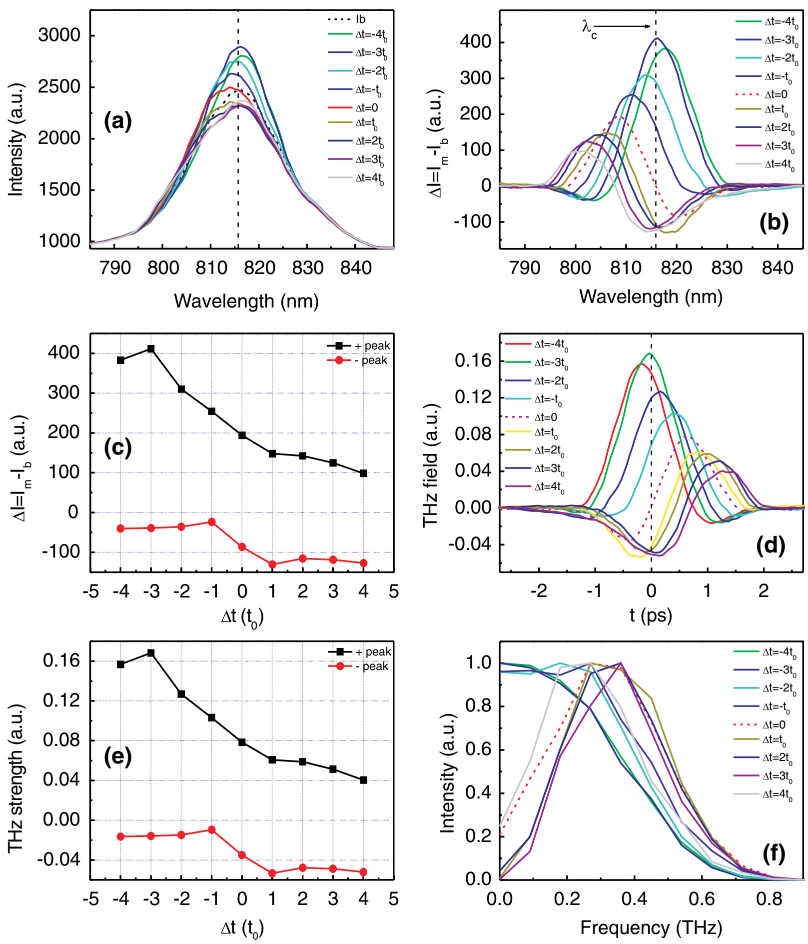

Fig. 5. (Color online) Experimental results of the THz signals measured with chirped probe pulse length ($T_c < T_{co}$) at different temporal discrepancy Δt. (a) Modulated spectra I_m versus background I_b at different Δt; (b) spectrum difference $\Delta I = I_m - I_b$ at different Δt; (c) the positive and negative peaks of spectrum difference ΔI at different Δt; (d) retrieved THz waveforms at different Δt; (e) the positive and negative peaks of retrieved THz waveforms at different Δt; (f) retrieved THz spectra at different Δt. In the experiment, $t_0 = 0.1334$ ps. The vertical dashed lines in (a) and (b) indicate the central wavelength λ_c of the background probe spectrum I_b.

whereas the temporal resolution is limited by the bandwidth of the probe beam (37 nm in our experiment) and the spectral resolution of our fiber spectrometer (~0.8 nm), which are the shortcomings of the spectral-encoding technique. Generally speaking, the higher the spectral resolution and the boarder the bandwidth of the probe pulse, the better the temporal resolution of the retrieved THz signal and the frequency resolution of the THz spectrum will be. In addition, the peak position and bandwidth of the THz spectrum of the THz emission from air-biased plasmas is dependent on the plasma densities (1 THz corresponding to $\sim 10^{16}/\mathrm{cm}^3$). These plasma densities can be controlled by changing the focusing pump laser intensity and the laser intensity can be changed with different focal lengths of the focusing lens and the pump laser energy. For example, in our experiment, we used a lens ($f/20$) to focus the pump laser and the main THz emission fell in the range of 0–1 THz, and the peak located at ~0.3 THz in the spectrum. Therefore, we did not consider the additional distortion due to the Fourier components outside the sampled frequency range (0–3 THz in ZnTe crystal).

4. DISCUSSION

Our simulation and experimental results indicate that imperfect synchronization between the probe and the THz pulse would introduce distortion when the THz signal is measured with the spectral-encoding technique. This distortion is dependent upon the shape of the THz waveform. For the symmetric bipolar THz signal with the same amplitude for its positive and negative polars, the distortion due to imperfect synchronization is very small if the temporal discrepancy $|\Delta t|$ is less than the THz pulse characteristic length T, as shown in Fig. 1(f). The retrieved THz spectrum shows a redshift. For the asymmetrical bipolar THz waveform, this distortion is more sensitive and severe under the same temporal discrepancy. The retrieved THz spectrum shows redshift if $\Delta t < 0$ or blueshift if $\Delta t > 0$. The distortion showing redshift or blueshift in the retrieved THz spectrum for any THz signals originates because the probe spectrum is not modulated by the whole field of the THz signal in the EO crystal if the probe pulse is not synchronized perfectly with the TH pulse. Hence, only part of the THz signal is recorded by the spectrometer. In addition, if a probe pulse with its length less than the optimal probe pulse duration is applied, this distortion will be amplified, as shown in Fig. 3(c).

To minimize the distortion from imperfect synchronization between the probe and THz pulses, the key issue is how to judge if the probe pulse is synchronized exactly with the THz pulse from the probe spectrum. Our simulation results indicate that the strongest signal is not a good criterion for judging if the probe pulse is synchronized perfectly with the THz pulse. For a symmetric bipolar THz signal, the judgment is not difficult, while for a THz signal with an arbitrary waveform, this judgment becomes more difficult. Generally speaking, the perfect synchronization between the probe and THz pulses is not far from the point of the strongest THz signal observed with the spectrometer. Here we propose a simple approach to realize perfect synchronization: first, find out the central wavelength from the background probe spectrum. Set the central wavelength line as the dashed vertical line shown in the simulations and experimental results described above, such as in Figs. 1(b), 2(b), 3(a), 3(d), and 5(b). Second, scan the THz signal from the spectrum difference $\Delta I = I_m - I_b$ in real time quickly by moving the probe delay line to obtain a full impression of the THz waveform shape and find out the strongest signal position. Third, adjust carefully the delay line to move the signal back and forth and make sure that the central wavelength line λ_c is located at the center of the curve of the spectrum difference ΔI. At this delay point, the probe pulse could be thought synchronized perfectly with the THz pulse.

It should be noted that both the distortion due to imperfect synchronization and the distortion from the strong THz signal (modulation depth $k \ll 1$ is not satisfied) have similar features in the THz frequency spectrum. In the former case, a significant rise toward lower frequencies and a slight pressing toward higher frequencies can be observed when the temporal discrepancy between the probe and THz pulses increases. In the latter case, the same phenomena can be observed if the THz field becomes stronger and stronger. However, these two kinds of distortion have different origins in nature. The former originates from the fact that only part of the signal is detected by the probe pulse due to the imperfect synchronization between them, while the latter comes from the neglect of the quadratic term of the modulation depth k, which reflects the strength of the THz signal in the retrieving process.

5. CONCLUSION

We demonstrated the behavior of the distortion of the THz signals due to imperfect synchronization between the chirped probe and THz pulses measured with the spectral-encoding technique by numerical simulation and experiment. It is found that this imperfect synchronization can affect the retrieved THz spectrum, especially the distribution of the lower frequency part if the temporal discrepancy is large. The distortion becomes more prominent when the probe pulse length is less than the optimal probe pulse duration. A distortion similar to the simulation results was observed in our experiments when the THz signals from a high-voltage-biased air plasma filament were measured. A simple approach to minimize this distortion was proposed.

ACKNOWLEDGMENTS

This work is supported in part by A*STAR Grant No. 0921540097 in Singapore and by the National Natural Science Foundation of China (NSFC, Grant Nos. 10734130 and 10874113) and the National Basic Research Program of China (Grant Nos. 2007CB310406, 2007CB815100, and 2009GB105002).

REFERENCES

1. Q. Wu and X.-C. Zhang, "7 terahertz broadband GaP electro-optic sensor," Appl. Phys. Lett. **70**, 1784–1786 (1997).
2. Z. Jiang and X.-C. Zhang, "Electro-optic measurement of THz field pulses with a chirped optical beam," Appl. Phys. Lett. **72**, 1945–1947 (1998).
3. Z. Jiang, F. G. Sun, and X.-C. Zhang, "Terahertz pulse measurement with an optical streak camera," Opt. Lett. **24**, 1245–1247 (1999).
4. B. Yellampalle, K. Y. Kim, G. Rodriguez, J. H. Glownina, and A. J. Taylor, "Algorithm for high-resolution single-shot THz measurement using in-line spectral interferometry with chirped pulses," Appl. Phys. Lett. **87**, 211109 (2005).
5. K. Y. Kim, B. Yellampalle, G. Rodriguez, R. D. Averitt, A. J. Taylor, and J. H. Glownia, "Single-shot, interferometric,

high-resolution, terahertz field diagnostic," Appl. Phys. Lett. **88**, 041123 (2006).
6. J. Shan, A. S. Weling, E. Knoesel, L. Bartels, M. Bonn, A. Nahata, G. A. Reider, and T. F. Heinz, "Single-shot measurement of terahertz electromagnetic pulses by use of electro-optic sampling," Opt. Lett. **25**, 426–428 (2000).
7. S. P. Jamison, J. Shen, A. M. MacLeod, W. A. Gillespie, and D. A. Jaroszynski, "High-temporal-resolution, single-shot characterization of terahertz pulses," Opt. Lett. **28**, 1710–1712 (2003).
8. K. Y. Kim, B. Yellampalle, A. J. Taylor, G. Rodriguez, and J. H. Glownia, "Single-shot terahertz pulse characterization via two-dimensional electro-optic imaging with dual echelons," Opt. Lett. **32**, 1968–1970 (2007).
9. Y. Kawada, T. Yasuda, A. Nakanishi, H. Takahashi, and S. Aoshima, "Single-shot measurement of terahertz temporal waveform using pulse-front tilting by a direct vision dispersion prism," Rev. Sci. Instrum. **80**, 113703 (2009).
10. U. Schmidhammer, V. De Waele, J.-R. Marquès, N. Bourgeois, and M. Mostafavi, "Single shot linear detection of 0.01–10 THz electromagnetic fields," Appl. Phys. B **94**, 95 (2009).
11. F. G. Sun, Z. Jiang, and X.-C. Zhang, "Analysis of terahertz pulse measurement with a chirped probe beam," Appl. Phys. Lett. **73**, 2233–2235 (1998).
12. J. R. Fletcher, "Distortion and uncertainty in chirped pulse THz spectrometers," Opt. Express **10**, 1425–1430 (2002).
13. X.-Y. Peng, O. Willi, M. Chen, and A. Pukhov, "Optimal chirped probe pulse length for terahertz pulse measurement," Opt. Express **16**, 12342–12349 (2008).
14. X.-Y. Peng, R. Jung, T. Toncian, O. Willi, and H.-T. Teng, "Distortion of the intense terahertz signal measured by spectral-encoding technique," Appl. Phys. Lett. **94**, 221107 (2009).
15. X.-Y. Peng, J.-H. Teng, X.-H. Zhang, and Y.-L. Foo, "Distortion analysis of pulsed terahertz signal measured with spectral-encoding technique," J. Appl. Phys. **108**, 093112 (2010).
16. A. Houard, Y. Liu, B. Prade, V. T. Tikhonchuk, and A. Mysyrowicz, "Strong enhancement of terahertz radiation from laser filaments in air by a static electric field," Phys. Rev. Lett. **100**, 255006 (2008).
17. Y. Chen, T.-J. Wang, C. Marceau, F. Théberge, M. Châteauneuf, J. Dubois, O. Kosareva, and S. L. Chin, "Characterization of terahertz emission from a dc-biased filament in air," Appl. Phys. Lett. **95**, 101101 (2009).